A Higher-Order Active Contour Model for Tree Detection[*]

Péter Horváth[1,2], Ian Jermyn[2], Zoltan Kato[1], Josiane Zerubia[2]

[1]University of Szeged, Institute of Informatics, P.O. Box 652, H-6701 Szeged, Hungary,
Email:{hp, kato}@inf.u-szeged.hu

[2]Ariana (joint research group CNRS/INRIA/UNSA), INRIA, B.P. 93, 06902 Sophia Antipolis, France,
Email:{Ian.Jermyn, Josiane.Zerubia}@sophia.inria.fr

Abstract

We present a model of a 'gas of circles', the ensemble of regions in the image domain consisting of an unknown number of circles with approximately fixed radius and short range repulsive interactions, and apply it to the extraction of tree crowns from aerial images. The method uses the recently introduced 'higher order active contours' (HOACs), which incorporate long-range interactions between contour points, and thereby include prior geometric information without using a template shape. This makes them ideal when looking for multiple instances of an entity in an image. We study an existing HOAC model for networks, and show via a stability calculation that circles stable to perturbations are possible for constrained parameter sets. Combining this prior energy with a data term, we show results on aerial imagery that demonstrate the effectiveness of the method and the need for prior geometric knowledge. The model has many other potential applications.

1. Introduction

The present paper has two purposes. First, to extend the range of the recently introduced higher-order active contour (HOAC) framework for region and image modelling [8] by introducing a model for a 'gas of circles', the ensemble of regions in the image domain consisting of an unknown number of circles with approximately fixed radius and short range repulsive interactions; and second, to apply this model to a problem of current interest in remote sensing image processing: the extraction of tree crowns. Forestry services (for example, the French National Forest Inventory (IFN)) are interested in various quantities associated with forests and plantations, such as the density of trees,

the mean crown area and diameter, and so on. This information is very useful for the management of resources and the conservation of forestry areas. The tree crown extraction problem is of importance because it can provide this information at a reasonable price. Field surveys or semi-automatic extraction of the necessary information from images is expensive.

Our model for tree crown extraction will consist of two parts: a likelihood energy E_i describing the image to be expected given a particular region corresponding to tree crowns; and a prior energy E_g describing the geometry of the regions corresponding to tree crowns. The latter will be a HOAC energy. HOACs [8, 9] are a new generation of active contour models [5]. While classical active contours use only boundary length and interior area (and perhaps boundary curvature) as prior knowledge, HOACs allow the incorporation of non-trivial prior knowledge about region geometry, and the relation between region geometry and the data, via nonlocal interactions between tuples of contour points. They are intrinsically Euclidean invariant. They differ from most other methods for incorporating prior geometric knowledge into active contours [2, 3, 6] in not being based upon perturbations of a reference region or regions. In consequence, they can detect multiple instances of an entity at no extra cost, a critical requirement for the current application.

The prior energy E_g will strongly favour regions consisting of an unknown number of approximate circles of roughly the same radius. To define this energy, we will adapt the existing HOAC models of network-shaped regions [6, 8]. One of the key properties of these models is the existence of a repulsive force between anti-parallel tangent vectors that prevents the 'arms' of the network region from collapsing to zero width. We exploit this repulsive interaction in order to create stable circles, but in doing so we wish to prevent the formation of the 'arms' that generate network-shaped regions. This requires a stability analysis of the energy in order to ensure that circles of a given radius

are stable to small perturbations of their boundaries, and that they have low energy. The latter condition means that circles are relatively easy to create, given supporting image data. The conditions place constraints on the parameters of the model. The same prior energy may also be useful in a broad range of other applications: *e.g.* the extraction of craters, missile silos, etc. in remote sensing.

In section 1.1, we recall the nature of HOAC energies. In section 2, we describe the proposed HOAC model for tree extraction, and present the stability analysis of the geometric term. In section 2.2, we describe a simple data term combining intensity and gradient information. In section 3, we present extraction results on real aerial images.

1.1. Higher order energies

Classical active contour energies are constructed from single integrals over the contour, meaning that they can only incorporate local differential-geometric information about the contour. In contrast, HOACs include multiple integrals over the contour. These integrals correspond to long-range interactions between tuples of contour points, and allow the incorporation of sophisticated prior geometric knowledge. Combined with length and area terms, one of the basic forms of Euclidean invariant quadratic HOAC models [8] is

$$E_g(\gamma) = \lambda L(\gamma) + \alpha A(\gamma)$$
$$- \frac{\beta}{2} \iint dp\, dp'\, \mathbf{t}(p) \cdot \mathbf{t}(p')\, \Phi(R(p, p')) , \quad (1.1)$$

where γ is the contour, parameterized by p; L is the length of the contour; A is its interior area; $R(p, p') = |\mathbf{R}(p, p')|$, where $\mathbf{R}(p, p') = \gamma(p) - \gamma(p')$; $\mathbf{t} = \dot{\gamma}$ is the tangent vector to the contour; and Φ is an interaction function that determines the geometric content of the model. We will take this function to be

$$\Phi(x) = \begin{cases} \frac{1}{2}(2 - \frac{x}{d_{\min}} + \frac{1}{\pi}\sin(\pi\frac{x}{d_{\min}})) & x \le d_{\min} , \\ 0 & x > d_{\min} , \end{cases} \quad (1.2)$$

as in [6, 8], where equation (1.1) was used to model network-shaped regions composed of thin arms that meet at junctions. Via the stability analysis in section 2.1, we will adjust the parameters of this model so that the low energy configurations are not networks, but approximate circles of approximately fixed radius.

2. Model for circle detection

Our model for tree crown extraction is of the form $E(\gamma, I) = E_i(I, \gamma) + E_g(\gamma)$. The likelihood energy E_i is described in section 2.2. In the first part of this section, we analyze the prior energy E_g, and show how it can be used to model a 'gas of circles'. We want to adjust the parameters of the model so that configurations consisting of collections of circles of approximately a certain radius r_0 are stable, and have low energy. Stability means that if the shape of a circle of radius r_0 is changed slightly, it will relax back into the circle. We will thus choose parameters so that a circle of radius r_0 is a minimum of E_g. To do so, we expand the energy in a Taylor series to second order in perturbations around a circle of radius r_0. We will then adjust the parameters so that the first derivative is zero, which tells us that the circle is an energy extremum, and so that the second derivative is positive definite, which tells us that the extremum is a minimum. The parameters can be further adjusted so that the energy of the minimizing circle is not too high.

2.1. Stability analysis

We want to calculate $E_g(\gamma) = E_g(\gamma_0 + \delta\gamma)$ to second order in $\delta\gamma$, where γ_0 is a circle of radius r_0. Since we are expanding around a circle, it is easiest to use polar coordinates (r, θ), and to choose $\theta(p) = p$ as the parameterization. Tangential changes $\delta\theta$ can be undone by a diffeomorphism and hence do not affect the energy. The radial perturbation δr can be expanded in a Fourier series on the circle:

$$\delta r(p) = \sum_k a_k e^{ikr_0 p} \qquad k = m/r_0, m \in \mathbb{Z} ,$$

where $a_k \ll r_0$. We can then express $L(\gamma)$ and $A(\gamma)$ to second order as

$$L(\gamma) = 2\pi r_0 \left\{ 1 + \frac{a_0}{r_0} + \frac{1}{2}\sum_k k^2|a_k|^2 \right\} \quad (2.1a)$$

$$A(\gamma) = \pi r_0^2 + 2\pi r_0 a_0 + \pi \sum_k |a_k|^2 . \quad (2.1b)$$

Note that stability for finite r_0 cannot be achieved with these terms alone. Setting the linear term to zero gives $\lambda = -r_0\alpha$. Substituting in the quadratic term reveals that either very low or very high frequencies are unstable, depending on the sign of λ.

The expansion of the quadratic term in equation (1.1) is of course more complicated, since we have to expand $\mathbf{t}$, R and Φ, but invariance with respect to translations around the circle means that the second-order term is diagonal in the Fourier basis. The result (details can be found in [4]), after combination with equations (2.1), is that the prior energy is given to second-order by

$$E_g(\gamma_0 + \delta\gamma) = E_0 + a_0 E_1 + \frac{1}{2}\sum_k |a_k|^2 E_2(k) ,$$

where

$$E_0 = 2\pi\lambda r_0 + \pi\alpha r_0^2 - \pi\beta \int_0^{2\pi} dp\, F_{00}$$

$$E_1 = 2\pi\lambda + 2\pi\alpha r_0 - 2\pi\beta \int_0^{2\pi} dp\, F_{10}$$

$$E_2 = 2\pi\lambda r_0 k^2 + 2\pi\alpha$$
$$- 2\pi\beta\Bigg[\Bigg(2\int_0^{2\pi} dp\, F_{20} + \int_0^{2\pi} dp\, F_{21}e^{ikr_0 p}\Bigg)$$
$$+ k\Bigg(2ir_0\int_0^{2\pi} dp\, F_{23}e^{ikr_0 p}\Bigg)$$
$$+ k^2\Bigg(r_0^2\int_0^{2\pi} dp\, F_{24}e^{ikr_0 p}\Bigg)\Bigg]. \qquad (2.2)$$

The F are functions of p and r_0, and depend on Φ. For example,

$$F_{10}(p, r_0) = r_0\cos(p)\big(\Phi(X_0) + r_0\left|\sin\tfrac{p}{2}\right|\dot\Phi(X_0)\big),$$

where $X_0 = 2r_0\left|\sin\tfrac{p}{2}\right|$. The other expressions are given in [4]. In order to achieve an extremum, the linear term must be zero. This implies that

$$\beta(\lambda, \alpha, r_0) = \frac{\lambda + \alpha r_0}{\int_0^{2\pi} dp\, F_{10}}, \qquad (2.3)$$

which fixes β given λ, α, and r_0. We set $\lambda = 1.0$ without loss of generality. Given r_0, we therefore have only two free parameters (the other is $d_{\min}$) to adjust to achieve stability, *i.e.* to make E_2 positive for all k. In figure 1(a), we plot β versus r_0 and α for $d_{\min} = 4$. A given r_0 defines a slice of the surface, the potentially stable pairs of (α, β), but only those pairs for which $E_2 \geq 0$ for all k are actually stable. Figure 1(b) shows the plot of E_0 for one such pair. Note that it has a minimum at r_0, so that it is stable against radial perturbations ($k = 0$). It is also stable with respect to perturbations with $k \neq 0$. Figure 2 shows experiments using just the prior energy, starting from various initial conditions, illustrating the formation of circles of the desired radius.

2.2. Data term and energy minimization

Having constructed a suitable prior energy, E_g, we must now couple the contour to the data. We use the likelihood energy

$$E_i(\gamma) = \lambda_i \int dp\, \mathbf{n}(p) \cdot \partial I(p)$$
$$+ \int_{\Omega_{in}} d^2x\, \frac{(I(x) - \mu_{in})^2}{2\sigma_{in}^2} + \int_{\Omega_{out}} d^2x\, \frac{(I(x) - \mu_{out})^2}{2\sigma_{out}^2},$$

where $\Omega_{in,out}$ are the interior and exterior regions of the contour, and I is the image. The first term is a standard gradient
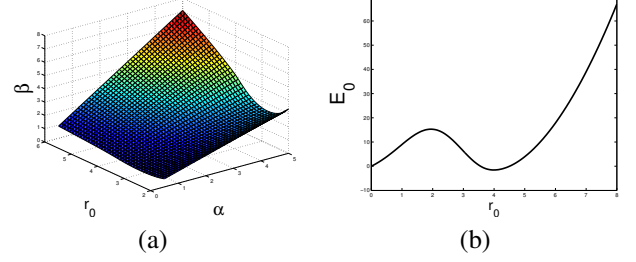

(a) (b)

Figure 1. (a): plot of β against α and r_0 from equation (2.3) ($d_{\min} = 4$); (b): plot of E_0 versus r for $\alpha = 1.0$, $\beta = 0.96$, and $r_0 = 4.0$.
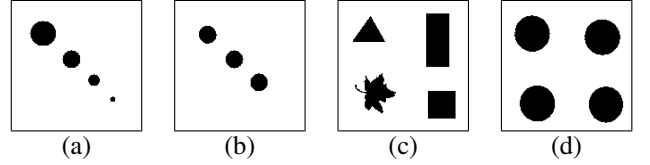

(a) (b) (c) (d)

Figure 2. Formation of stable circles, (b) and (d), with $r_0 = 10$ and 20 respectively, from two different initial conditions, (a) and (c).

flux term, while the other terms, first used in an active contour context by [1], model the classes 'inside' and 'outside' as white Gaussian noise around a mean. We note that the normalization constant for this likelihood can be expressed in terms of the length and interior area of the contour, and the parameters μ and σ. These parameters are learned initially from examples of each of the classes using maximum likelihood, and then fixed. We therefore do not include the normalization constant explicitly, since it amounts to a simple change in the parameters λ and α, and we are interested in stability of the posterior in the absence of image-dependent terms. If μ and σ were estimated during gradient descent, it would be important to include the normalization constant explicitly, since it depends on these parameters.

The energy is minimized by gradient descent starting from a generic initialization: a rounded rectangle just smaller than the image domain. The functional derivatives of all except the quadratic term are standard. The functional derivative of the quadratic term gives rise to a gradient descent force given by

$$\hat{\mathbf{n}} \cdot \frac{\partial\gamma}{\partial\tau}(p) = \beta \int dp'\, \hat{\mathbf{R}}(p, p') \cdot \mathbf{n}(p')\dot\Phi(R(p, p')), \quad (2.4)$$

where $\mathbf{n}$ is the outward-pointing normal vector, and $\hat{\mathbf{R}} = \mathbf{R}/R$. To evolve the contour we use the level set framework [7] extended to the demands of nonlocal forces such
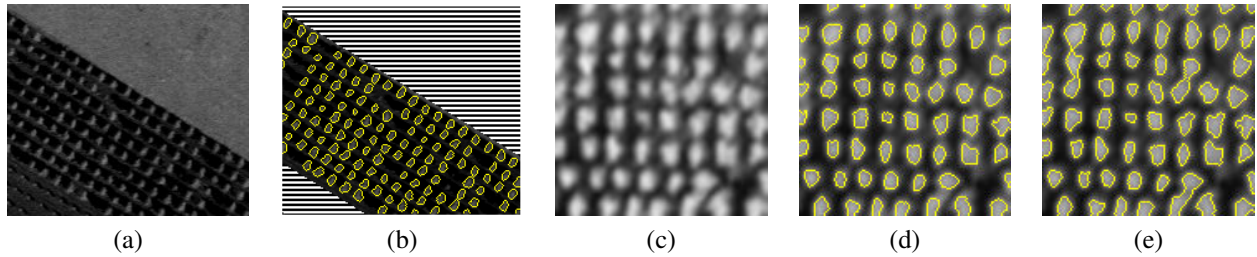
Figure 3. a and c: aerial images of plantations (©️ IFN); b and d: corresponding segmentation results ((b): $\alpha = 1.0, \beta = 0.96, \lambda = 1.0, r_0 = 4.0$**; (d):** $\alpha = 5.8, \beta = 4.6, \lambda = 1.0, r_0 = 6.0$**); e: the best result with** $\beta = 0$**.**

as equation (2.4) [8].

3. Experimental results

Here we present extraction results on 54 cm/pixel aerial images of plantations located in Saône et Loire in France. (For references to other techniques applied to the same problem see [4].) Figure 3(a) shows a regularly planted poplar stand. The tree crowns are $\sim$ 8–10 pixels in diameter, *i.e.* $\sim$ 4–5m. The result is shown in figure 3(b). We have applied the algorithm only in the central part of the image; we do not deal with the dashed areas. Figure 3(c) shows a small piece of an irregularly planted poplar forest. The image is difficult because the intensities of the crowns are very varied, some trees overlap, and the gradients are blurred. The result is shown on figure 3(d). From the results, it is simple to calculate various properties of the tree plantation: number of trees, total area, density, and so on.

The consequences of setting $\beta = 0$, thereby reducing the model to a standard active contour with length and area terms, are shown in figure 3(e), which shows the best result obtained in this case. Note that several trees that are in reality separate are merged into single regions, and the shapes of trees are often rather distorted, whereas the prior geometric knowledge included when $\beta \neq 0$ allows the separation of the trees and the regularization of their shapes.

4. Conclusion

The incorporation of prior geometric knowledge in models of regions is critical for many applications, particularly when quasi-automatic operation is required. In this paper, we have described a higher-order active contour model of a 'gas of circles', which favours regions consisting of a number of disjoint components, each of which is roughly circular and of a certain radius. We have shown the importance of this prior knowledge by applying the model to the extraction of tree crowns from high resolution remote sensing images. Many other applications in remote sensing and other domains can be envisaged.

References

[1] T. F. Chan and L. A. Vese. Active contours without edges. *IEEE Trans. Image Processing*, 10(2):266–277, 2001.

[2] D. Cremers, T. Kohlberger, and C. Schnörr. Shape statistics in kernel space for variational image segmentation. *Pattern Recognition*, 36(9):1929–1943, sep 2003.

[3] A. Foulonneau, P. Charbonnier, and F. Heitz. Geometric shape priors for region-based active contours. *Proceedings of the IEEE International Conference on Image Processing*, 3:413– 416, 2003.

[4] P. Horvath, I. H. Jermyn, J. Zerubia, and Z. Kato. Higher-order active contour model of a 'gas of circles' and its application to tree detection. Research report, INRIA, France. To appear.

[5] M. Kass, A. Witkin, and D. Terzopoulos. Snakes: Active contour models. *Int. J. Comp. Vis.*, 1(4):321–331, 1988.

[6] M. Leventon, W. Grimson, and O. Faugeras. Statistical shape influence in geodesic active contours. In *Proceedings of the IEEE International Conference on Computer Vision and Pattern Recognition*, volume 1, pages 316–322, Hilton Head Island, South Carolina, USA, 2000.

[7] S. Osher and J. A. Sethian. Fronts propagating with curvature dependent speed: Algorithms based on Hamilton-Jacobi formulations. *Journal of Computational Physics*, 79(1):12–49, 1988.

[8] M. Rochery, I. H. Jermyn, and J. Zerubia. Higher order active contours and their application to the detection of line networks in satellite imagery. In *Proc. IEEE Workshop Variational, Geometric and Level Set Methods in Computer Vision*, at ICCV, Nice, France, Oct. 2003.

[9] M. Rochery, I. H. Jermyn, and J. Zerubia. Higher order active contours. *International Journal of Computer Vision*, 2006. In press.